

Sample Rate Conversion with Fluctuating Resampling Ratio

Marek Blok

Faculty of Electronics, Telecommunications and Informatics
Gdańsk University of Technology
11/12 G. Narutowicza Street, 80-233 Gdańsk, Poland
e-mail: mblok@eti.pg.gda.pl

Piotr Drózda

ADVA Optical Networking Sp. z o.o
35/37 Śląska Street, 81-310 Gdynia, Poland
e-mail: PDrozda@advaoptical.com

ABSTRACT — In this paper a sample rate conversion with continuously changing resampling ratio has been presented. The proposed implementation is based on variable fractional delay filter implemented using a Farrow structure. It has been demonstrated that using the proposed approach instantaneous resampling ratio can be freely changed. This allows for simulation of audio recorded on magnetic tape with nonuniform velocity as well as removal of these distortions using the same algorithm.

I. INTRODUCTION

A huge number of sample rate standards [1] available today create a demand on development of sample rate conversion (SRC) algorithms [2]–[4]. The digital resampling algorithm replaces digital-analog conversion followed by analog signal sampling allowing for more flexible implementations. A common example used to demonstrate usefulness of such algorithms is the conversion between compact disc (CD) with $F_s = 44.1$ kHz (multimedia standard) and digital tape (DAT) with $F_s = 48$ kHz (communications standard) [3], [5]. In this paper we present SRC implementation based on variable fractional delay (VFD) filter. Using this algorithm we not only can implement an arbitrary constant resampling ratio but fluctuating changes in resampling ratio can be readily implemented as well. Based on this tool we propose a novel application for resampling algorithm which is correction of signals with unintentional nonuniform sampling. For example correction of old recordings with distortions resulting from nonuniform velocity of the media [6]–[8] which is typically addressed with interpolation techniques [9]. On the other hand, with correctly sampled signal we might simulate such distortions using the same VFD SRC algorithm. In both cases, we make use of the fact that nonuniformly sampled signal when reconstructed with uniform sampling changes its pitch inversely proportionally to the sample rate changes.

II. VFD FILTER

The SRC algorithm investigated in this paper is based on FD filters and its performance depends on the design method used to calculate coefficients of FD filter. In this paper to the approximate ideal FD filter the FIR FD filter with the frequency response

$$H_N(f) = \sum_{n=0}^{N-1} h[n] \exp(-j2\pi fn) \quad (1)$$

is used where $h[n]$ is the impulse response of the length N . The designer tries to find the coefficients of this impulse response which offer the best performance of FD filter, which is usually evaluated using frequency domain error function [10]

$$E(f) = H_N(f) - H_{id}(f) \quad (2)$$

where the ideal frequency response $H_{id}(f)$ of the FD filter with total delay τ_d is defined by the following formula [10]

$$H_{id}(f) = \exp(-j2\pi f\tau_d), \quad f \in [-0.5, 0.5) \quad (3)$$

which corresponds to the ideal impulse response

$$h_{id}[n] = \text{sinc}(n - \tau_d) \quad (4)$$

Because of the causality requirement, high performance FD filters are characterized with nonzero integer delay $D = \text{round}(\tau_d)$, which for FIR filters is usually selected close to the bulk delay $\tau_N = (N - 1)/2$. With those two delays defined, we receive the following formula for the total delay

$$\tau_d = D + d = \tau_N + \varepsilon \quad (5)$$

where $d \in [-0.5, 0.5)$ is the fractional delay and ε is the net delay.

There are several design methods offering optimal FD filters with maximally flat (MF), least squares (LS) and minimax being the most popular methods. The optimality criteria for each of these methods is based on complex approximation error (2). For MF filters approximation error and its $N - 1$ derivatives must be equal to zero. The MF filter offers excellent performance but only around zero frequency. Differently, the LS and minimax filters allow the designer to specify the approximation band $f \in [0, f_a]$ in which the error is minimized. The LS FD filter [10] has the energy of error minimized

$$E_{LS}(f_a) = 2 \int_0^{f_a} |E(f)|^2 df \quad (6)$$

while the minimax FD filter [10], [11] has minimized peak error (PE)

$$E_{PE}(f_a) = \max_{f \in [0, f_a]} |E(f)| \quad (7)$$

in the approximation band.

The coefficients of the impulse response, vector \mathbf{h} , of all these optimal filters, MF, LS and minimax, with fractional delay d can be found solving the following matrix equation [10]

$$\mathbf{P}\mathbf{h} = \mathbf{p} \quad (8)$$

where the coefficients of matrix \mathbf{P} and vector \mathbf{p} depend on the optimization criteria. For MF filter matrix \mathbf{P} is a Vandermonde matrix

$$\mathbf{P}_{k+1,n+1} = n^k \quad (9)$$

and vector \mathbf{p} has elements

$$\mathbf{p}_{1,k+1} = \tau_d^k \quad (10)$$

where $k, n = 0, 1, \dots, N - 1$. To find the LS filter we need only to change coefficients of matrix \mathbf{P}

$$\mathbf{P}_{k+1,n+1} = f_a \operatorname{sinc} f_a(n - k) \quad (11)$$

and column vector \mathbf{p}

$$\mathbf{p}_{1,k+1} = f_a \operatorname{sinc} f_a(k - \tau_d) \quad (12)$$

A minor modification is needed for minimax filters. First a set of $N + 1$ frequency points f_k , called extremal points, must be found using recursive complex Remez algorithm [12]. Then coefficients of matrix \mathbf{P} and vector \mathbf{p} can be computed using the following formulas

$$\mathbf{P}_{k+1,n+1} = \cos(2\pi f_k n) - \sin(2\pi f_k n) \quad (13a)$$

$$\mathbf{p}_{k+1,N+1} = (-1)^k \quad (13b)$$

and

$$\mathbf{p}_{1,k+1} = \cos(2\pi f_k \tau_d) - \sin(2\pi f_k \tau_d) \quad (14)$$

where $k = 1, 2, \dots, N + 1$ and $n = 1, 2, \dots, N$. In this case vector \mathbf{h} has one additional element with magnitude equal to peak approximation error (7).

Since VFD filter needs to be able to change its delay for each output sample the high numerical costs related to solving matrix equation (8) become a significant problem. The most popular solution is the Farrow structure [11], [13]–[15]. The idea of this structure is to approximate each sample of the impulse response with a separate polynomial of the order q dependent on fractional delay d

$$h[n] = \sum_{m=0}^q c_m[n] d^m \quad (15)$$

Now, the output samples of the FD filter can be expressed with the following formula

$$y[n] = \sum_{k=0}^{N-1} h[n] x[n - k] = \sum_{m=0}^q y_m[n] d^m \quad (16)$$

here

$$y_m[n] = \sum_{k=0}^{N-1} c_m[k] x[n - k] \quad (17)$$

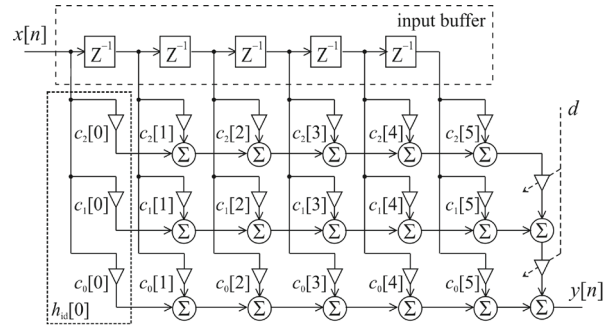


Fig. 1. Farrow structure of the order $q = 2$ implementing VFD filter of the length $N = 5$.

Formulas (16) and (17) define the Farrow structure presented in Fig. 1 where each row coefficients implement separate filter with impulse response $c_m[n]$.

To find coefficients $c_m[n]$ we need to compute only a few impulse responses of FD filters for fractional delays d uniformly spread in range $[-0.5, 0.5]$. In practice, to compute approximation polynomials it is enough to use just $q + 1$ impulse responses. The polynomials of order q equal to 6 or 7 offer performance adequate for high quality FD filters with approximation error about -100dB [11].

III. SAMPLE RATE CONVERSION USING VFD FILTER

Classic three rate sample rate conversion algorithm is presented in Fig. 2. Input signal samples with sample rate F_{s1} is up-sampled by means of insertion of $L - 1$ zeros between each pair of consecutive input samples. Next, at the intermediate sample rate, the lowpass interpolation filter with upper frequency $f_u = \min(0.5/L, 0.5/M)$ prevents the aliasing and removes spectral images resulting from zeroinserting. At last stage, the sample rate is reduced to the desired one by means of decimation, only every M -th sample remains in the output signal.

This approach, because of its simplicity, is well suited for simple cases requiring constant sample ratio with small factors L and M . In other cases the intermediate sampling ratio is very high and the passband of the interpolation filter becomes extremely narrow. In the result numerical costs increase drastically and, what's more important, the interpolation filter becomes very difficult to design. Therefore for arbitrary resampling ratios the VFD filter is used (Fig. 3).

As we can see in Fig. 4, the output sample $y[m]$ can be interpreted as the closest input sample delayed by a fraction of sampling period $d[m]$. This fractional delay can be computed

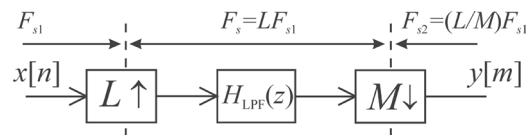


Fig. 2. Classic three-rate sample rate conversion algorithm by rational factor L/M .

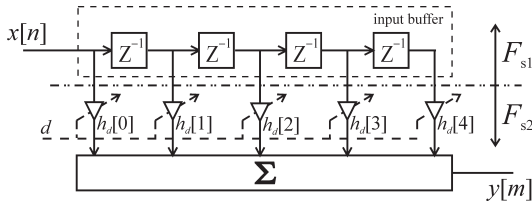


Fig. 3. General VFD filter structure applied to SRC.

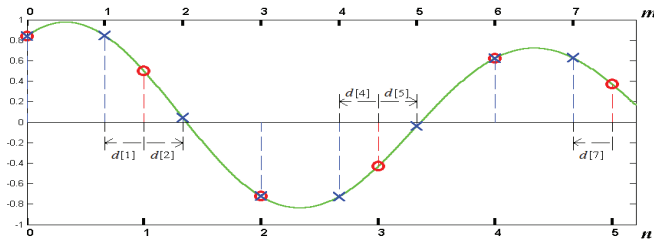


Fig. 4. Illustration of sample rate conversion by $L/M = 2/3$. Input samples $x[n]$ – o, output samples $y[m]$ – x.

using the following recursive formula [16]

$$d[m] = d[m - 1] - r[m] + \Delta n[m] \quad (18)$$

where the reversal of instantaneous resampling ratio

$$r[m] = F_{s1}[m]/F_{s2}[m] = T_{s2}[m]/T_{s1}[m] \quad (19)$$

and $\Delta n[m]$ is a number of new samples required in input buffer to compute the next output sample

$$\Delta n[m] = \text{round}(r[m] - d[m - 1]) \quad (20)$$

For rational resampling ratio (Fig. 2)

$$r[m] = M/L \quad (21)$$

sequences $d[m]$ and $\Delta n[m]$ are periodic with period L , but in general with VFD filter the resampling ratio can be an arbitrary positive number and can change in time. Nevertheless, if we want to avoid resampled signal distortions then $r[m]$ must be limited by the instantaneous signal oversampling ratio.

With the above two parameters defined ((18) and (20)) the resampling algorithm is following (Fig. 3):

- 1) start with $d[0] = 0$ and $\Delta n[0] = 0$,
- 2) wait for $\Delta n[m]$ new samples in input buffer,
- 3) find output sample $y[m]$ delayed by $d[m]$ using FD filter,
- 4) calculate $\Delta n[m]$ and $d[m]$ for next m and go back to step 2.

For every output sample the resampling algorithm requires different fractional delay (18). This means that for each output sample we need to compute a new impulse response of the FD filter. For rational resampling ratio L/M we actually need only L impulse responses which can be stored in look-up-table (LUT) [3] but when ratio is arbitrary and additionally changing in time, the filters needed in resampling cannot be specified beforehand and must be computed during runtime which can be done readily using Farrow structure presented in the previous section.

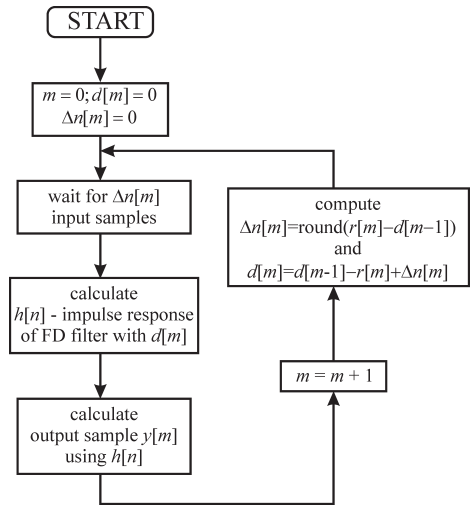


Fig. 5. Diagram of SRC algorithm based on VFD filter.

IV. FD FILTER DESIGN FOR SRC

If the best performance of SRC algorithm must be achieved then the optimal FD filters like minimax or LS [10], [12], [16] with approximation band specified by the designer seem to be the best option. Especially that with the Farrow structure the complexity of the FD filter design algorithm does not affect the runtime VFD filter implementation since all structure coefficients can be computed beforehand.

Nevertheless, we must notice that it is not sufficient to know just the errors of FD filters to assess the performance of the SRC algorithm based on these filters. It can be observed that the SRC algorithm based on FD filters (Fig. 3 and 5) is equivalent to the classic approach (Fig. 2) [16]. We only need to replace the interpolation filter in the classic approach with the overall filter which is composed of FD filters used in resampling [16]. This can be done only for rational resampling ratios but the conclusions can be readily adapted to arbitrary resampling ratios.

To obtain the impulse response of the overall filter [16] we need to interleave impulse responses $h_{d[m]}[n]$ of FD filters with fractional delays $d[m]$

$$h_o[m + nL] = h_{d[m]}[n]; \quad m = 0, 1, \dots, L - 1 \quad (22)$$

with delays $d[m]$ arranged in decreasing order

$$d[m - 1] = d[m] + 1/L; \quad m = 1, \dots, L - 1 \quad (23)$$

Using the overall filter (22) we can readily analyze distortions introduced by the SRC algorithm based on FD filters since this filter must fulfill the same requirements as the interpolation filter in the classic approach (Fig. 2).

In Fig. 6 we can see overall filter obtained for minimax FD filters with upper frequency of approximation band $f_a = 0.4$. The problem with the SRC based on optimal filters is that the overall filter demonstrates large lobes in stopband which may result in aliasing when input signal has components above f_a . Moreover, the transition band location of the overall filter

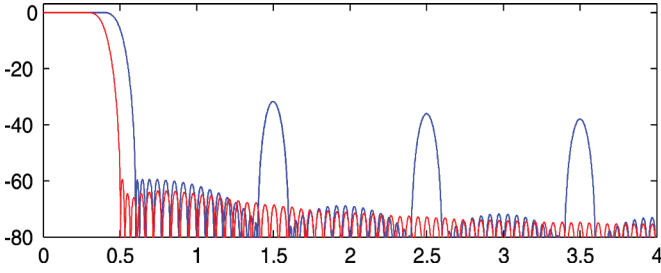


Fig. 6. Comparison of overall filters composed of minimax FD filters (blue) and composed of FD filters designed using offset window method (red) of the length $N = 17$ and with $f_a = 0.4$ and offsetting MF filter of the length $N_{\text{off}} = 5$ for $L = 9$.

cannot be manipulated. These disadvantages of optimal FD filter can be overcome with the use of offset window method [17]–[20]. Using filters designed with offset window method for window extracted from minimax filter, the large lobes in stopband are eliminated and the transition band can be readily shifted [20] (Fig. 6). The numerical cost of the VFD implementation do not change since, as we have observed, the Farrow structure of the same order can be used also in this case.

Although the overall filters in Fig. 6 are composed of just $L = 9$ filters their properties are maintained for any resampling ratio. An excellent testing signal for the SRC algorithm is the constant amplitude LFM chirp, which has been used in Fig. 7. We can see there that the signal converted using minimax FD filters demonstrates high distortions when input signal frequency exceeds f_a . On the other hand, the signal converted using FD filters designed with offset window has no components caused by nonlinear distortions larger than -60 dB which is directly related to the peak error (7) of the worst FD filter used in the SRC algorithm [16].

V. PROCESSING WITH FLUCTUATING RESAMPLING RATIO

In this section we will demonstrate SRC with changing ratio. The first simple yet spectacular example is the conversion of sinusoidal signal with constant frequency F_{in} into chirp signal with linear instantaneous frequency

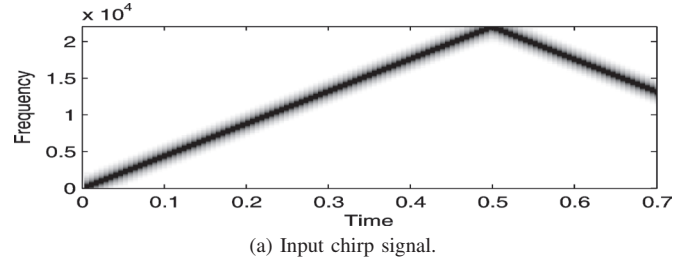
$$F_{out}[m] = F_0 + m\Delta F \quad (24)$$

where F_0 is the initial output sample rate and ΔF is the chirp rate. In this example the input sample rate is constant and the output sample rate must change in such a way that the oversampling ratio will change linearly according to output ne index m .

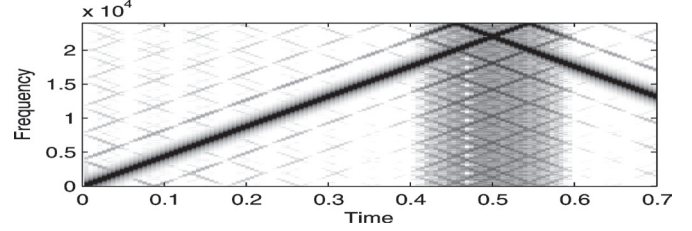
$$F_{s2}[m] = F_{in}\overline{F_{s2}}/F_{out}[m] \quad (25)$$

here $\overline{F_{s2}}$ is the constant output sample ratio required for sampled signal to observe chirp with assumed instantaneous frequency (24). Since in this example input sampling frequency F_{s1} is constant the formula for the reversal of the instantaneous resampling ratio can be readily obtained

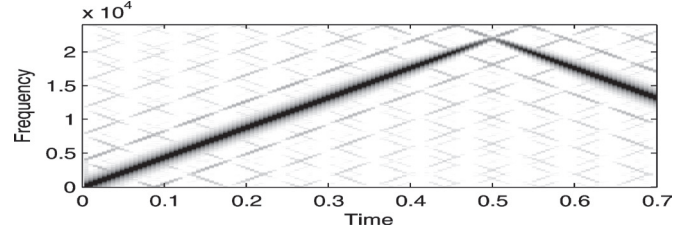
$$r_{\text{chirp}}[m] = F_{s1}/F_{s2}[m] = \frac{F_{in}(F_0 + m\Delta F)}{F_{s1}\overline{F_{s2}}} \quad (26)$$



(a) Input chirp signal.



(b) Chirp signal resampled using minimax FD filters.



(c) Chirp signal resampled using FD filters designed using window offset with MF filter of the length $N_{\text{off}} = 5$.

Fig. 7. Spectrograms illustrating resampling with constant resampling ratio 160/147. VFD filter of the length $N = 17$ and Farrow structure order $q = 5$.

The effects of resampling are presented in Fig. 9. Let us notice that when the output signal is reconstructed using variable output sample rate (25) the input (Fig. 9a) and output (Fig. 9c) signals represent the same analog signal. However, if we assume constant output rate $\overline{F_{s2}}$, the output samples of SRC algorithm represent the chirp signal (Fig. 9b) which we wanted to obtain.

The process described above can be reversed. The chirp signal obtained in the previous step can be converted back to sinusoid but selection of the $r[m]$ is now more difficult. In the first scenario the sample rate and the frequency of the input signal are constant which simplifies the derivations. In this problem we need to assume that either the frequency of the input signal or its sample rate is changing. Since we want to demonstrate how to reverse the resampling process we will assume that the signal frequency is constant with variable distance between input samples.

From (25) we know the sample ratio and input sampling instants but need to find the ratio $r[m]$ (19) specified in equidistant output instants m . Let us assume that we know the instantaneous input sample rate $F_{s1}[n] = 1/T_{s1}[n]$ sampled in the same instants as the input signal $x[n]$ and instantaneous output sample rate $F_{s2}[m] = 1/T_{s2}[m]$ sampled in the same instants as the output signal $y[m]$. We are looking for ratio $r[m] = T_{s2}[m]/\hat{T}_{s1}[m]$ where $\hat{T}_{s1}[m]$ is the input sampling

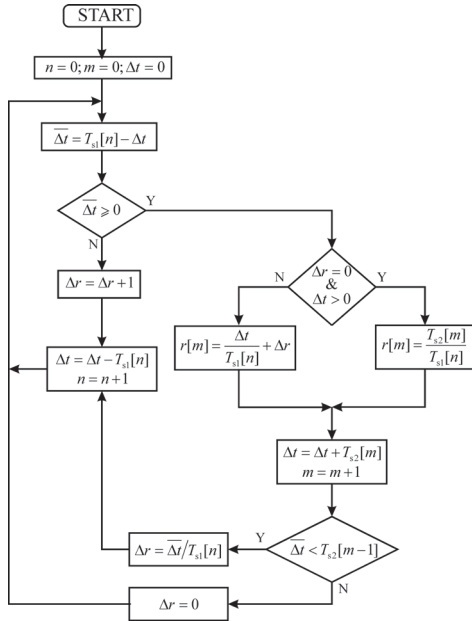


Fig. 8. Diagram for computation of $r[m]$ (19) based on instantaneous input and output sample rates.

period corresponding to the output time instant m .

Assuming that we know the positions of input sampling instants, which are our output instants from the previous problem

$$t_{in}[n] = \sum_{i=1}^n T_{s1}[n] = t_{in}[n-1] + T_{s1}[n] \quad (27)$$

and output sampling instants, which are our input instants from the previous problem

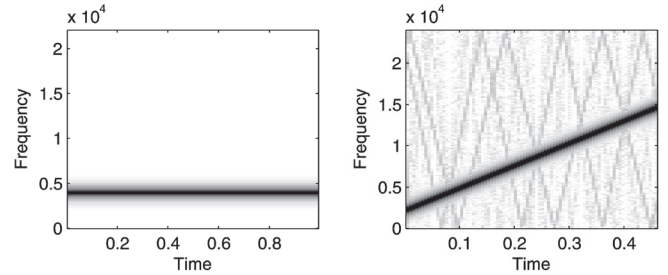
$$t_{out}[m] = \sum_{i=1}^m T_{s2}[m] = t_{out}[m-1] + T_{s2}[m] \quad (28)$$

We propose the following algorithm for computation of the reversal of the instantaneous resampling ratio $r[m]$.

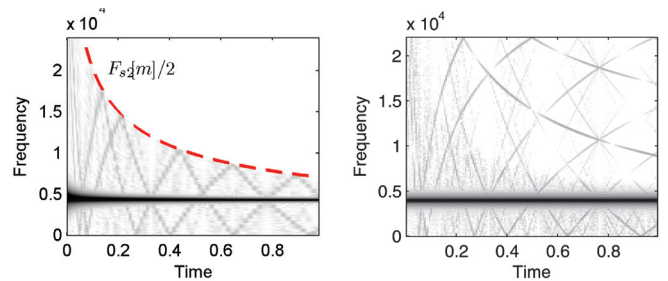
- 1) Start with input and output discrete time indexes $n := 0$ and $m := 0$ with corresponding continuous time instants $t_{in} := 0$ and $t_{out} := 0$.
- 2) Compute distance from the current output time instant to the current and the next input time instant:

$$\begin{aligned} \Delta t &:= t_{out} - t_{in}, \\ \overline{\Delta t} &:= T_{s1}[n] - \Delta t. \end{aligned}$$

- 3) If $\overline{\Delta t} \geq 0$ then
 - a) if the previous output sample is located in the same input sampling interval ($\Delta r = 0$ and $\Delta t > 0$) then $r[m] := T_{s2}[m]/T_{s1}[n]$, otherwise $r[m] := \Delta t/T_{s1}[n] + \Delta r$,
 - b) If $\overline{\Delta t} < T_{s2}[m]$ then $\Delta r := \overline{\Delta t}/T_{s1}[n]$ and move to the next input instant



(a) Spectrogram of input sinusoidal signal. (b) Spectrogram of chirp signal obtained from sinusoidal signal. Assumed constant sample rate $F_{s2} = F_{s1}$.



(c) Spectrogram from Fig. 9b reshaped with accordance to variable sample rate. Dashed line indicates the folding frequency. (d) Spectrogram of restored sinusoidal signal.

Fig. 9. Conversion from sinusoidal signal into chirp and back using SRC based on VFD filters. VFD filter with $f_a = 0.4$ of the length $N = 17$ and Farrow order $q = 5$ designed using window offset using MF FD filter of length $N_{off} = 5$.

$$\begin{aligned} t_{in} &:= t_{in} + T_{s1}[n], \\ n &:= n + 1, \end{aligned}$$

otherwise
 $\Delta r := 0$,

- c) move to the next output instant

$$\begin{aligned} t_{out} &:= t_{out} + T_{s2}[m], \\ m &:= m + 1, \end{aligned}$$

- 4) otherwise ($\overline{\Delta t} < 0$)

- a) $\Delta r := \Delta r + 1$,
- b) move to the next input instant

$$\begin{aligned} t_{in} &:= t_{in} + T_{s1}[n], \\ n &:= n + 1, \end{aligned}$$

- 5) Go to point 2.

The proposed algorithm is universal and can be used for computation of instantaneous ratio $r[m]$ for any variable input and output sample rates. Fig. 8 presents the modified version of the proposed algorithm. The introduced modifications allow to eliminate from algorithm the continuous accumulation of input and output times which eventually would lead to roundoff errors. In Fig. 9d spectrogram of sinusoidal signal recovered from chirp signal generated in previous example is presented. We can observe the nonlinear distortions but their level can be controlled with the selection of the overall filter (Fig. 6)

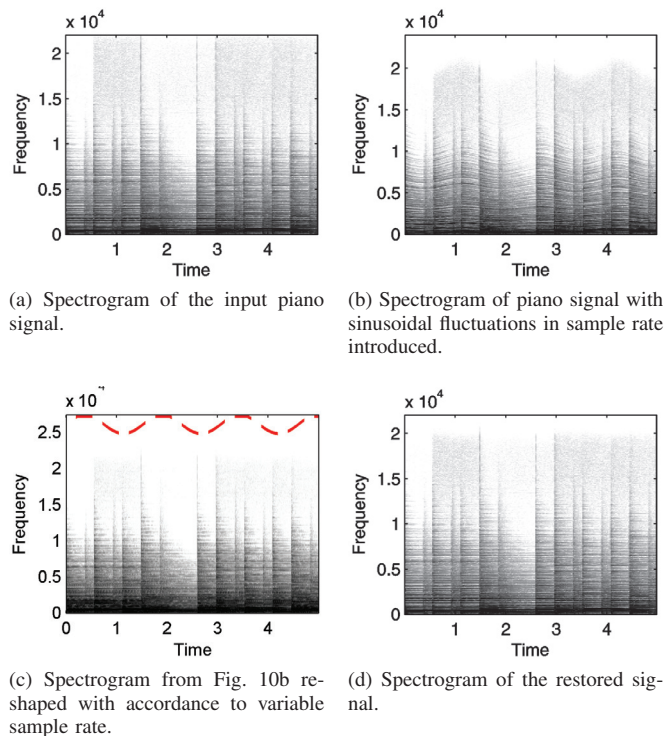


Fig. 10. Manipulations on piano music. Introduction and removal of sinusoidal fluctuations into instantaneous sample ratio. VFD filter with $f_a = 0.45$ of the length $N = 47$ and Farrow order $q = 6$ designed using window offset method using MF FD filter of length $N_{\text{off}} = 6$.

attenuation in the stopband.

Fig. 10 presents the example in which a sinusoidal sample rate changes are introduced and later removed from the processed signal. The signal contains the piano music sensitive to such distortions. Presented example simulates the case in which a velocity of magnetic tape changes because of mechanical problems. As we can see, the proposed solution can be used efficiently to remove such distortion if only we are able to find out how the velocity/sampling ratio changes [6]–[8].

VI. CONCLUSION

We have demonstrated that using Farrow structure implementing VFD filter audio signal can be resampled with continuously changing sample rate ratio. The proposed approach can be used to simulate signal distortions, for example change or remove speech intonation, as well as to correct old recordings distorted because of non-constant media velocity, e.g. magnetic tape.

In this paper we have only demonstrated that the proposed solution can be used in aforementioned applications. Further search should focus on comparison with other resampling methods and automatic selection on sample rate ratio based for example on changes of pitch period for speech processing or on the properties of recorded distortions for reconstruction of old recordings [6]–[8].

ACKNOWLEDGMENT

This work was in part supported by the Polish Ministry of Science and Higher Education under the research project financed from the state budget designated for science in the years 2010-2012.

REFERENCES

- [1] AES5-2008, "AES recommended practice for professional digital audio – preferred sampling frequencies for applications employing pulse-code modulation," Audio Engineering Society, Tech. Rep., 2008, revision of AES5-1997.
- [2] A. Tarczyski, W. Kozinski, and G. D. Cain, "Sampling rate conversion using fractional-sample delay," in *Proc. IEEE ICASSP'94*, Adelaide, Australia, May 1994, pp. 285–288.
- [3] E. Hermanowicz, M. Rojewski, and M. Blok, "A sample rate converter based on a fractional delay filter bank," in *Proc. ICSPAT 2000*, Dallas, Tx, USA, Oct. 16–19, 2000.
- [4] G. Evangelista, "Design of digital systems for arbitrary sampling rate conversion," *Signal Process.*, vol. 83, no. 2, pp. 377–387, Feb. 2003.
- [5] K. Rajamani, L. Yhean-Sen, and C. W. Farrow, "An efficient algorithm for sample rate conversion from CD to DAT," *IEEE Signal Process. Lett.*, vol. 7, no. 10, pp. 288–290, 2000.
- [6] A. Ciarkowski, A. Czyzewski, M. Dziubinski, A. Kaczmarek, B. Kostek, M. Kulesza, and P. Maziewski, "Methods for detection and removal of parasitic frequency modulation in audio recordings," in *AES Conference: 26th International Conference: Audio Forensics in the Digital Age*, Jul. 2005.
- [7] A. Czyzewski, A. Ciarkowski, A. Kaczmarek, J. Kotus, M. Kulesza, and P. Maziewski, "Dsp techniques for determining ŠwowŦ distortion," *J. Audio Eng. Soc.*, vol. 55, no. 4, pp. 266–284, 2007.
- [8] A. Czyzewski, P. Maziewski, and A. Kupryjanow, "Reduction of parasitic pitch variations in archival musical recordings," *Signal Processing*, vol. 90, no. 4, pp. 981 – 990, 2010.
- [9] P. Maziewski, "Wow defect reduction based on interpolation techniques," *Bulletin of the Polish Academy of Science: Technical Sciences*, vol. 54, pp. 469–477, 2006.
- [10] T. I. Laakso, V. Välimäki, M. Karjalainen, and U. K. Laine, "Splitting the unit delay — tools for fractional delay filter design," *IEEE Signal Process. Mag.*, vol. 13, no. 1, pp. 30–60, 1996.
- [11] M. Blok, "Farrow structure implementation of fractional delay filter optimal in Chebyshev sense," in *Proc. SPIE*, vol. 6159, Wilga, Poland, May 30 – Jun. 2, 2005, p. 61594K.
- [12] —, "Optimal fractional sample delay filter with variable delay," in *OSEE 2002*, TechOnLine, Bedford, Massachusetts, USA, Mar. 18, 2002. [Online]. Available: <http://www.eetimes.com/design/analog-design/4018005>
- [13] C. W. Farrow, "A continuously variable digital delay element," in *Proc. IEEE ISCAS'88*, Espoo, Finland, 1988, pp. 2641–2645.
- [14] F. J. Harris, "Performance and design of Farrow filter used for arbitrary resampling," in *Proc. DSP'97*, vol. 2, Santorini, Greece, 1997, pp. 595–599.
- [15] E. Hermanowicz, "On designing a wideband fractional delay filter using the Farrow approach," in *Proc. EUSIPCO'2004*, Austria, Sep. 6–10, 2004, pp. 961–964.
- [16] M. Blok, "Collective filter evaluation of an FSD filter-based resampling algorithm," in *OSEE 2002*, TechOnLine, Bedford, Massachusetts, USA, Jan. 15, 2002. [Online]. Available: www.eetimes.com/design/signal-processing-dsp/4017905
- [17] A. Yardim, G. D. Cain, and P. Henry, "Optimal two-term offset windowing for fractional delay," *Electron. Lett.*, vol. 32, no. 6, pp. 526–527, Mar. 1996.
- [18] A. Yardim, G. D. Cain, and A. Laverigne, "Performance of fractional-delay filters using optimal offset windows," in *Proc. IEEE ICASSP'97*, vol. 3, Apr. 21–24, 1997, pp. 2233–2236.
- [19] E. Hermanowicz, "A nearly optimal variable fractional delay filter with extracted Chebyshev window," in *Proc. IEEE ICECS'98*, vol. 2, Lisboa, Portugal, Sep. 7–10, 1998, pp. 401–404.
- [20] M. Blok, "Fractional delay filter design with extracted window offsetting," in *Proc. MixDes'2012*, Warsaw, Poland, May 24–26, 2012.